Article

Not peer-reviewed version

Physicochemical and Mechanical Characterization of HDPE and LDPE Films Used in the Postharvest Packaging of Banana (*Musa paradisiaca*)

Maritza D. Ruiz Medina * and Jenny Ruales

Posted Date: 15 September 2025

doi: 10.20944/preprints202509.1156.v1

Keywords: banana; postharvest packaging; polyethylene films; HDPE; LDPE; thermal analysis; FTIR; tensile properties; zinc migration

 doi:10.20944/preprints202509.1156.v1

Article

Physicochemical and Mechanical Characterization of HDPE and LDPE Films Used in the Postharvest Packaging of Banana (*Musa paradisiaca*)

Maritza D. Ruiz Medina * and Jenny Ruales

Departamento de Ciencias de Alimentos y Biotecnología (DECAB), Escuela Politécnica Nacional (EPN), Quito, 170143, Ecuador

* Correspondence: marilolita3@hotmail.com or maritza.ruiz@epn.edu.ec; Tel.: +593-62-609-240 or +593-997-666-999

Abstract

The postharvest preservation of banana (*Musa paradisiaca*) is essential to maintain fruit quality, reduce losses, and ensure consumer acceptability during storage and distribution. Packaging films play a critical role in protecting fruit from mechanical damage and environmental stress while extending shelf life. This study compared the physicochemical and mechanical properties of two widely used polyethylene films—high-density polyethylene (HDPE) and low-density polyethylene (LDPE)—under simulated postharvest conditions. Films were characterized by Differential Scanning Calorimetry (DSC), Fourier Transform Infrared Spectroscopy (FTIR), Thermogravimetric Analysis (TGA), and Flame Atomic Absorption Spectroscopy (AAS) for trace element detection. Structural integrity was assessed by macro- and microphotography, while tensile tests quantified mechanical performance. Results showed that HDPE presented higher melting stability, crystallinity, and tensile strength, with detectable zinc content (0.82–0.94 mg/100 g), whereas LDPE was zinc-free but exhibited greater flexibility. Both materials retained their polyethylene chemical fingerprint without oxidative degradation, although LDPE displayed more pronounced surface deterioration after weathering (288, 864, and 1440 h). These findings highlight HDPE's superior stability and safety for banana export packaging, while emphasizing the importance of monitoring potential trace element migration to ensure compliance with food-contact regulations and sustainability in tropical fruit supply chains.

Keywords: banana; postharvest packaging; polyethylene films; HDPE; LDPE; thermal analysis; FTIR; tensile properties; zinc migration

1. Introduction

Banana (*Musa paradisiaca*), one of the most consumed tropical fruits, plays a pivotal role in global trade and food security, particularly in Latin America, Africa, and Southeast Asia [1]. Its dual role as a staple food and export commodity underscores its socioeconomic importance, contributing to rural employment and income generation. However, as a climacteric fruit characterized by high respiration rates and ethylene production, bananas are highly perishable and prone to mechanical damage, dehydration, microbial infection, and rapid postharvest deterioration [2,3]. Postharvest banana losses often reach critical levels in producing countries due to inadequate handling practices and the use of inefficient packaging technologies [4].

To mitigate these losses, polymeric plastic packaging, particularly polyethylene (PE)—has become a widely adopted strategy to protect bananas, delay ripening, and maintain their sensory and physicochemical quality during storage and distribution [3]. PE films offer multiple advantages, including light weight, flexibility, transparency, affordability, and adjustable barrier properties [5]. Research further shows that antifungal coatings combined with PE packaging can reduce respiration rates and microbial spoilage, thereby preserving fruit quality [6]. Among the

 doi:10.20944/preprints202509.1156.v1

main variants, low-density polyethylene (LDPE) and high-density polyethylene (HDPE) are the most used materials in fruit packaging. These polymers differ considerably in molecular structure, crystallinity, permeability, and mechanical behavior, which can influence their suitability for postharvest conservation [7,8].

Despite their widespread application, the underlying mechanisms by which packaging extends banana shelf life remain under investigation [9]. For example, vacuum packaging has been shown to reduce crown rot incidence by below 3% compared with over 50% in unpackaged controls during cold storage [5], while microperforated compostable LDPE films retained fruit quality for up to 30 days at 14 °C [10]. Similarly, the application of myo-inositol delayed ethylene biosynthesis and enhanced antioxidant mechanisms, prolonging shelf life [11,12]. However, chilling injury, characterized by lignification and oxidative stress, remains a major limitation during low-temperature storage [6]. Reviews emphasize that edible coatings combined with LDPE or HDPE packaging reduce gas exchange and moisture loss, particularly when formulated with antioxidants or antimicrobials [13]. Moreover, mechanization of postharvest operations, such as field de-handing, can enhance packaging efficiency and reduce labor dependence [14].

Nevertheless, there is still limited research directly comparing LDPE and HDPE under postharvest conditions specific to *Musa paradisiaca* [1]. Most studies have focused on fruit quality outcomes such as shelf life, firmness, or color changes, with less attention to the intrinsic physicochemical and mechanical properties of packaging materials [1,15,16]. Recent investigations highlight differences in crystallinity, permeability, and tensile strength between PE variants, which may affect their effectiveness in protecting climacteric fruits [17]. At the same time, environmental and food safety considerations—including additive migration [18], polymer thermal resistance [18,19], and recyclability or degradability [8]—are becoming increasingly relevant in packaging science.

Advanced analytical techniques provide a comprehensive evaluation of polymer performance. Differential Scanning Calorimetry (DSC) determines melting temperature, onset of melting, and enthalpy of fusion, directly linked to crystallinity and stability under cold storage [20,21]. DSC has been applied to polymer composites and debris characterization, proving sensitive to crystallinity changes and useful in diagnostic contexts [22–24]. Thermogravimetric Analysis (TGA) quantifies mass loss, decomposition temperatures, and residues, providing insight into integrity under humidity and thermal stress [25]. Fourier Transform Infrared Spectroscopy (FTIR) identifies functional groups, additives, and degradation by-products, with studies on oxo-biodegradable PE confirming oxidative chain scission [25–28]. Atomic Absorption Spectroscopy (AAS) enables trace metal detection in food-contact polymers, supporting risk assessment of elements like Cd, Pb, and Zn [29–31].

Mechanical and structural characterization also contributes to understanding packaging performance. Tensile testing evaluates tensile strength, elongation at break, and Young's modulus, reflecting the balance between resistance and flexibility under handling stress [32,33]. Macro- and microphotography document defects such as cracks or delamination that may compromise barrier function [33]. Similar approaches have been applied to edible protein-based films [34], biopolymer packaging [35], and recycled PE films, where microscopy has correlated structural changes with declining mechanical properties [36–38]. Innovations include dual-layer active films and nanocomposite systems with enhanced durability [39].

Degradability is another critical factor affecting recyclability and environmental performance of PE films. Accelerated weathering studies demonstrate structural and chemical modifications that influence service life [40–42]. Multi-technique analyses reveal the release of degradation by-products during photo-aging [43–45], while recycling studies indicate that reprocessed LDPE may retain mechanical integrity [40,46,47]. Such evaluations predict patterns of degradation, aging, and durability across storage periods, bridging laboratory findings with real supply-chain conditions [3,48,49]. Comparative studies show that HDPE generally retains strength and barrier performance longer than LDPE [44,47,50], suggesting that HDPE may be more suitable for cold-chain export, while LDPE provides handling flexibility at the cost of greater environmental sensitivity [33,50].

Therefore, this study aimed to conduct a comprehensive physicochemical and mechanical characterization of HDPE and LDPE films used in the postharvest packaging of banana (*Musa paradisiaca*) [5,51,52]. The materials were evaluated using DSC, FTIR, TGA, AAS, tensile testing, and macro- and microphotography. The findings provide insights into the performance, stability, and

 doi:10.20944/preprints202509.1156.v1

safety of these materials, supporting improved postharvest management, reducing fruit losses, and contributing to the development of more sustainable packaging practices [53–55]. In addition, the findings are contextualized within emerging research on biodegradable and nanocomposite packaging systems, which have demonstrated the ability to prolong banana shelf life, modulate ethylene production, and enhance overall sustainability in postharvest management [56–58]

2. Materials and Methods

2.1. Sample Collection and Treatment

Banana (*Musa paradisiaca*) fruits at commercial maturity stage 1 were harvested in May 2024 from farms located in El Oro province, Ecuador. Fruits showing visible defects or mechanical injuries were excluded. Upon arrival at the Department of Food and Biotechnology (DECAB), the fruits were washed with distilled water and air-dried at room temperature.

A coating formulation was prepared using food-grade ingredients: whey, cassava starch, agar, and glycerol, supplemented with 400 ppm of cinnamon essential oil (*Cinnamomum verum*) for antifungal activity. The mixture was homogenized under magnetic stirring to ensure uniform dispersion of all components. The coating was applied by immersion, covering the entire fruit surface, and bananas were dried under ambient conditions for 12–15 min [59–61].

Following drying, bananas were individually packaged in two types of polyethylene films obtained from commercial suppliers: low-density polyethylene (LDPE) and high-density polyethylene (HDPE). The films had an average thickness of 0.10 ± 0.01 mm, measured with a digital caliper. Packaged fruits were stored under controlled conditions at 13 ± 1 °C and 95% relative humidity in a cold chamber.

To evaluate the combined effect of the antifungal coating and polyethylene packaging on banana preservation, eight treatments were established. The experimental design included initial controls (0 h) and progressive storage intervals of 288, 864, and 1440 h (≈12, 36, and 60 days), which were selected as evaluation points for monitoring the physicochemical, mechanical, and structural performance of the fruits and packaging. A detailed description of the treatments is provided in Table 1.

Table 1. Description of treatments combining antifungal coating and polyethylene packaging types.

Code	Polyethylene type	Exposure time (h)	Condition / Series
T01	HDPE (high-density)	0	Initial control
T02	HDPE (high-density)	288	≈12 days
T03	HDPE (high-density)	864	≈36 days
T04	HDPE (high-density)	1440	≈60 days
T05	LDPE (low-density)	0	Initial control
T06	LDPE (low-density)	288	≈12 days
T07	LDPE (low-density)	864	≈36 days
T08	LDPE (low-density)	1440	≈60 days

2.2. Physicochemical Characterization

2.2.1. Atomic Absorption Spectroscopy (AAS)

Zinc (Zn) content in the polyethylene films was quantified by Flame Atomic Absorption Spectroscopy (AAS) using a PerkinElmer Analyst 200 spectrometer (PerkinElmer, Waltham, MA, USA), operated under the conditions recommended in the Analytical Methods for Atomic Absorption Spectrometry. Calibration curves were prepared with certified zinc standards (Merck, Darmstadt, Germany) in the range of 0.2–1.0 mg/L, and quality control samples were used to validate accuracy [29].

Sample digestion followed the procedure described in the Analytical Methods for Atomic Absorption Spectrometry (PL-1 Analysis of Polyethylene). Approximately 10 g of each polymer film was slowly calcined in a porcelain crucible until complete ashing of the organic fraction. The

 doi:10.20944/preprints202509.1156.v1

crucibles were then placed in a muffle furnace at 800 °C for 30 min. After cooling, 0.9 g of sodium carbonate (Na_2CO_3, analytical grade, Ecuador) was added and heated until the carbonate was fully melted [29].

Once cooled to room temperature, 7 mL of sulfuric acid (H_2SO_4, 3 M, analytical grade, Ecuador) was carefully added to dissolve the residue, and the crucible was rinsed thoroughly. The solution was then transferred to a 10 mL volumetric flask and diluted to volume with H_2SO_4 3 M [29].

All laboratory glassware and crucibles were pre-cleaned with acetone (analytical grade, Ecuador), followed by sequential rinses with nitric acid (0.1 M and 6.5%, analytical grade, Ecuador) to minimize contamination. Results were expressed as mg Zn/100 g of film. The measurements were carried out in triplicate (n=3) using independent digestions for each sample type, and results are reported as mean ± standard deviation.

2.2.2. Differential Scanning Calorimetry (DSC)

The thermal behavior of polyethylene films was evaluated using a differential scanning calorimeter (DSC Netzsch 204 F1 Phoenix, Netzsch, Germany). Approximately 5–6 mg of each sample were weighed with an analytical balance (Denver Instrument Company AA-200) and sealed in standard aluminum pans. The tests were carried out under a nitrogen atmosphere (99% purity) to prevent oxidative degradation [23].

The experimental procedure followed ASTM D3418 (ASTM International, West Conshohocken, PA, USA) [62]. Each specimen was subjected to a first heating cycle from 25 °C to 200 °C at a constant rate of 10 °C·min^{-1}, followed by a 10 min isothermal stage. Samples were then cooled to room temperature at the same rate and subjected to a second heating cycle under identical conditions. The first heating cycle was used to eliminate the thermal history of the films, whereas the parameters reported corresponded to the second heating cycle [24].

From the DSC thermograms, the melting temperature (Tm), onset of melting (Tonset), and enthalpy of fusion (ΔHf) were determined. The degree of crystallinity (Xc) was calculated using a reference enthalpy of fusion for 100% crystalline polyethylene (ΔH° = 293 J·g^{-1}). Each treatment was analyzed in three independent specimens (n = 3), and the results are expressed as mean ± standard deviation [50].

2.2.3. Fourier Transform Infrared Spectroscopy (FTIR)

The chemical structure of HDPE and LDPE films was analyzed by Fourier Transform Infrared Spectroscopy (FTIR) at 0, 288, 864, and 1440 h of storage under cold-chain conditions (13 °C, 95% RH). Analyses were performed on a Bruker Alpha II spectrometer equipped with an Attenuated Total Reflectance (ATR) diamond crystal module, following ASTM E1655-17 [26,28].

Spectra were acquired in the range of 4000–500 cm^{-1} with a resolution of 4 cm^{-1}, averaging 32 scans per sample. All spectra were background-corrected, and a mild baseline adjustment was applied to improve comparability. For figure presentation only, light smoothing was applied; however, all calculations were performed on unsmoothed, baseline-corrected spectra [26].

The polyethylene fingerprint was monitored at the characteristic CH_2 stretching (2916 and 2848 cm^{-1}), bending (1471 and 1462 cm^{-1}), and rocking (730 and 720 cm^{-1}) vibrations. Oxidation markers were evaluated in the carbonyl region (1700–1730 cm^{-1}) relative to the methylene scissoring band at 1462 cm^{-1}. Crystalline order was assessed through the intensity ratio of the rocking doublet at ~730/720 cm^{-1} [5,37].

Results are presented as overlay plots across 4000–600 cm^{-1} to compare functional group positions and intensities, and as focused windows on the 800–680 cm^{-1} and 1700–1740 cm^{-1} regions to highlight crystallinity and potential oxidation changes, respectively [37]. Instrument settings and background acquisitions were kept constant throughout the analysis to ensure reproducibility and comparability across polymers and storage times.

 doi:10.20944/preprints202509.1156.v1

2.2.4. Thermogravimetric Analysis (TGA)

Thermogravimetric analysis was carried out according to ASTM E1131 using a TA Instruments Q500 system equipped with a platinum pan and automated mass/temperature calibration. Film specimens (8–10 mg) were die-cut from the central area of each sheet to avoid edge effects and defects. For each exposure condition (0, 288, 864, and 1440 h) and polymer type (HDPE, LDPE) [25,27].

An empty-pan baseline was recorded prior to each run to correct for buoyancy and instrumental drift. Samples were equilibrated at 50 °C for 10 min, then heated from 50 to 900 °C at 10 °C·min^{-1} under high-purity nitrogen (99.999%) flowing at 60 mL·min^{-1}. To quantify non-volatile residue (e.g., inorganic additives or contaminants), an additional oxidative step was performed at 900 °C for 20 min by switching the purge gas to air at the same flow rate [27].

Raw mass-loss curves (mass % vs. temperature) were exported at 1–2 °C intervals. Derivative thermogravimetry (DTG) was obtained by numerical differentiation using a Savitzky–Golay smoothing filter (21-point window, second-order polynomial) to enhance peak readability without altering temperature values [5,25]. From the TGA/DTG curves, the following parameters were extracted: (i) T_5% and T_{95}% (temperatures at 5% and 95% mass loss), (ii) T_{50}% (midpoint of decomposition), (iii) Tonset (extrapolated onset) and Tmax (DTG peak temperature), and (iv) residual mass at 900 °C (and ash after the oxidative step). Results are reported as mean ± SD (n = 3) and visualized as 2D overlay plots and 3D surfaces (temperature × exposure time × mass loss) with T_5%, T_{50}%, and T_{95}% markers highlighted.

2.3. Structural and Mechanical Characterization

2.3.1. Macro- and Microphotography

HDPE and LDPE bags were analyzed under conditions: (0, 288, 864 y 1440 horas). From each condition, flat specimens of approximately 70 × 70 mm were cut and conditioned at 23 ± 2 °C for at least 30 min prior to imaging. Samples were placed on a matte black background to highlight cracks, surface defects, and textures [33,36].

Photographic documentation was carried out using a Sony Alpha 9 digital camera equipped with a Sigma Sport 70–200 mm f/2.8 DG DN lens, mounted on a tripod. The focal length was set at 70 mm, and the exposure parameters were: aperture f/9, exposure time 1/20 s, and ISO 100. A 5-s shutter delay was applied to avoid vibration. Images were captured in RAW format and subsequently converted into PNG files for further processing and analysis.

Illumination was provided by two high-CRI (≥ 95) LED light sources positioned at 45° relative to the sample plane and diffused through translucent panels to minimize specular reflections. An additional grazing light (~20°) was used to emphasize microtextures, extrusion marks, and surface defects induced by use.

Microstructural analysis of the polyethylene films was performed using a Nikon Eclipse E200 compound microscope (DECAB, EPN). Samples of HDPE and LDPE bags were collected at 0 h (unused control) and after 288, 864, and 1440 h of use as banana packaging. For each condition, film pieces of approximately 2 × 2 cm were cut and mounted flat on glass slides, with edges fixed using adhesive tape to avoid curling [63].

Observations were carried out under bright-field transmitted illumination at 40× magnifications. Images were acquired with a Nikon Digital Sight camera system controlled by NIS-Elements software and exported in TIFF/PNG format.

For each storage interval, at least three representative fields per sample were recorded, covering both general views and localized defects. The analysis focused on documenting surface texture, extrusion marks, microcracks, delamination zones, and other features associated with environmental exposure, mechanical stress, or polymer relaxation.

This methodology provided complementary evidence to macrophotography, allowing the detection and quantification of microstructural changes associated with storage and weathering in HDPE and LDPE packaging films.

 doi:10.20944/preprints202509.1156.v1

2.3.2. Tensile Testing

Uniaxial tensile properties of the polyethylene films were determined in accordance with ASTM D882. For each polymer (HDPE, LDPE) and storage time (0, 288, 864, 1440 h), rectangular strips were die-cut with a CEAST punch to 120 mm × 10 mm (length × width) along the machine direction to maintain orientation. Film thickness was measured at three locations with a digital micrometer; the average value was used for stress calculations.

Tests were carried out on an Instron universal testing machine (model 1011) fitted with flat grips and a 5 kN load cell. The initial grip separation was 70 mm and the crosshead speed was 500 $mm \cdot min^{-1}$, consistent with ASTM D882 for the thickness range of these films. Experiments were conducted under laboratory conditions (23 ± 2 °C). For each condition, n = 10 specimens were tested to enable reporting of mean values and standard deviations.

Young's modulus (E) was calculated from the initial linear region (0.05–0.25% strain), while maximum tensile strength (σ_max) and elongation at break (ε_b) were obtained at the peak load and at rupture, respectively. Results are reported as mean ± standard deviation for each polymer and exposure time.

3. Results

3.1. Atomic Absorption Spectroscopy (AAS)

Zinc (Zn) was analyzed in the polyethylene films at the initial stage (0 h). Among the two treatments tested, T01 (HDPE, initial control) showed detectable Zn concentrations, ranging from 0.82 to 0.94 mg/100 g, with an average of 0.93 ± 0.05 mg/100 g (n = 3). In contrast, T05 (LDPE, initial control) presented Zn concentrations below the limit of quantification (LC = 0.006 mg/100 g).

These results demonstrate that Zn was only detected in the HDPE film, likely due to the incorporation of Zn-based additives or catalysts during manufacturing. The absence of Zn in LDPE (T05) indicates greater consistency with food-contact safety standards. Although the Zn level in T01 was low, its detection underlines the importance of monitoring trace metals in packaging materials used for banana export.

3.2. Differential Scanning Calorimetry (DSC)

The second heating cycle revealed clear differences in the thermal behavior of HDPE and LDPE films subjected to accelerated weathering (Table 2). HDPE exhibited consistently higher melting temperatures (Tm = 129.8–137.5 °C) compared with LDPE (Tm = 118.6–125.4 °C), confirming its greater crystalline stability. Onset temperatures (Tonset) followed the same trend, remaining close to Tm in all cases.

The enthalpy of fusion (ΔHf) and crystallinity (Xc), calculated using a conservative baseline approach, showed variable responses across exposure times. In HDPE, ΔHf dropped sharply at 864 h (0.15 ± 0.08 J/g; Xc = 0.05 ± 0.03%), indicating severe structural rearrangements, and partially recovered at 1440 h (1.40 ± 0.55 J/g; Xc = 0.48 ± 0.19%). In contrast, LDPE displayed a more stable profile, with ΔHf reaching a maximum of 2.35 ± 0.95 J/g (Xc = 0.80 ± 0.32%) at 864 h before decreasing moderately at 1440 h (1.15 ± 0.65 J/g; Xc = 0.39 ± 0.22%).

Overall, the DSC analysis demonstrates that HDPE maintains higher melting stability than LDPE throughout the study, although its crystalline decreases significantly under prolonged exposure. LDPE, while less crystalline overall, exhibited more gradual and less pronounced structural changes.

Table 2. Differential Scanning Calorimetry (DSC) parameters of HDPE and LDPE films after 0, 288, 864, and 1440 h of weathering.

Polyethylene type	Exposure time (h)	Condition / Series	Tm (°C)	Tonset (°C)	ΔHf (J/g)	Xc (%)

 doi:10.20944/preprints202509.1156.v1

T01	HDPE (high-density)	0	Initial control	130.0 ± 1.5	128.0 ± 1.0	3.20 ± 0.50	1.09 ± 0.17
T02	HDPE (high-density)	288	≈12 days	129.8 ± 1.2	128.5 ± 1.1	3.05 ± 0.90	1.04 ± 0.31
T03	HDPE (high-density)	864	≈36 days	137.5 ± 2.5	136.9 ± 2.8	0.15 ± 0.08	0.05 ± 0.03
T04	HDPE (high-density)	1440	≈60 days	132.7 ± 2.1	131.1 ± 2.6	1.40 ± 0.55	0.48 ± 0.19
T05	LDPE (low-density)	0	Initial control	118.6 ± 2.1	116.9 ± 2.0	1.40 ± 0.80	0.48 ± 0.27
T06	LDPE (low-density)	288	≈12 days	123.7 ± 0.9	122.3 ± 1.0	1.55 ± 0.75	0.53 ± 0.25
T07	LDPE (low-density)	864	≈36 days	125.4 ± 1.6	123.6 ± 1.7	2.35 ± 0.95	0.80 ± 0.32
T08	LDPE (low-density)	1440	≈60 days	123.4 ± 0.8	122.0 ± 0.7	1.15 ± 0.65	0.39 ± 0.22

The DSC thermograms (Figure 1) showed distinct melting transitions for HDPE and LDPE films at 0 and 1440 h of storage. At the initial stage, HDPE exhibited a melting peak at 130.0 °C, which shifted slightly to 132.7 °C after 1440 h, confirming its higher crystalline stability. LDPE presented lower melting temperatures, increasing from 118.6 °C at 0 h to 123.4 °C at 1440 h. These results demonstrate that HDPE consistently maintained higher thermal stability compared with LDPE, while both polymers displayed moderate shifts in melting behavior after prolonged exposure.

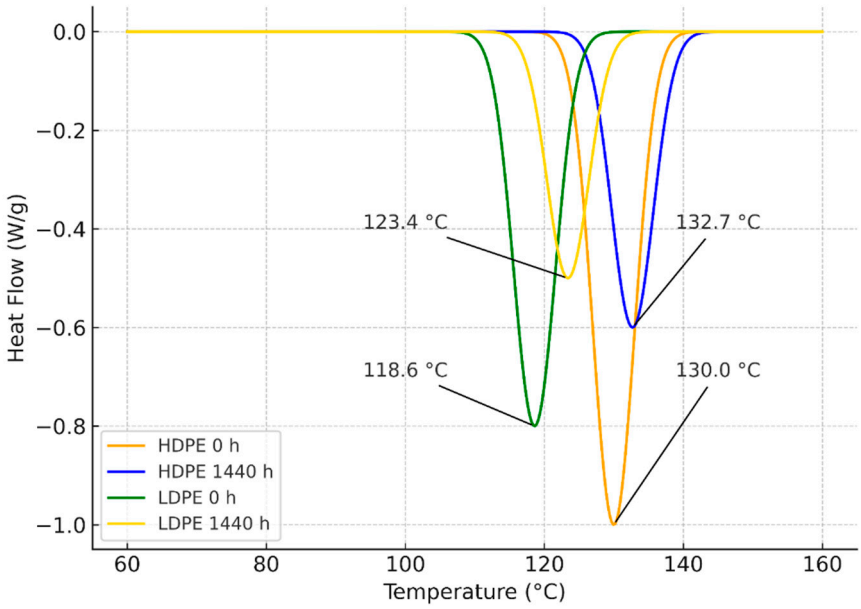

Figure 1. Representative DSC thermograms of HDPE and LDPE plastic films used for banana (Musa paradisiaca) preservation at 0 h and 1440 h of weathering under storage conditions.

3.3. Fourier Transform Infrared Spectroscopy (FTIR)

The FTIR spectra of HDPE and LDPE films (T01–T08) exhibited the characteristic polyethylene fingerprint throughout the storage period (0–1440 h), with no evidence of new functional groups. All spectra consistently showed: (i) strong methylene stretching bands at ~2918 and ~2848 cm^{-1}

 doi:10.20944/preprints202509.1156.v1

(ν_as(CH_2), ν_s(CH_2)), (ii) methylene bending at ~1472 and ~1463 cm^{-1} (δ(CH_2)), and (iii) the orthorhombic rocking doublet at ~730/720 cm^{-1} (ϱ_r(CH_2)). No carbonyl absorption was detected in the 1700–1740 cm^{-1} region, indicating negligible oxidative formation of C=O groups within the method's detection limits. Similarly, no distinct vinyl signals (~910–990 cm^{-1}) were observed. A summary of the main FTIR band assignments and their stability over time is provided in Table 3.

Band positions remained essentially constant across exposure times, and relative intensities varied only within experimental noise. In HDPE (T01–T04), the 730/720 cm^{-1} doublet—commonly used as a qualitative marker of crystalline ordering—did not exhibit systematic broadening or loss of intensity, which is consistent with DSC findings of high melting stability and only moderate reductions in fusion enthalpy at prolonged storage. LDPE (T05–T08) also preserved its polyethylene spectral profile with minimal shifts, confirming structural stability during the test period.

Overall, FTIR corroborates that the chemical backbone of both HDPE and LDPE remained intact throughout storage and that the structural rearrangements suggested by DSC are attributable to crystalline reorganization rather than oxidative degradation.

Table 3. FTIR spectral assignments for polyethylene films (HDPE and LDPE) and observed changes across storage times.

Wavenumber (cm^{-1})	Assignment	Observation across time
~2918, ~2848	ν_as/ν_s(CH_2)	Stable positions and relative intensities in all series.
~1472, ~1463	δ(CH_2) (scissoring)	Stable; used as internal reference for qualitative indices.
~730, ~720	ϱ_r(CH_2) (orthorhombic)	Doublet preserved; no systematic loss—consistent with modest crystallinity changes.
1700–1740	C=O (carbonyl)	**Not detected**; Carbonyl Index effectively ~0 within noise.
910–990	=CH_2 / vinyl	Not evident; no unsaturation growth.

The evolution of the orthorhombic rocking doublet (~730/720 cm^{-1}), commonly used as a qualitative marker of crystallinity in polyethylene, is shown in Figure 2. Spectra of HDPE and LDPE films recorded between 800 and 680 cm^{-1} at different storage times (0, 288, 864, and 1440 h) reveal that the characteristic doublet remained preserved throughout the experiment, with only minor variations in intensity.

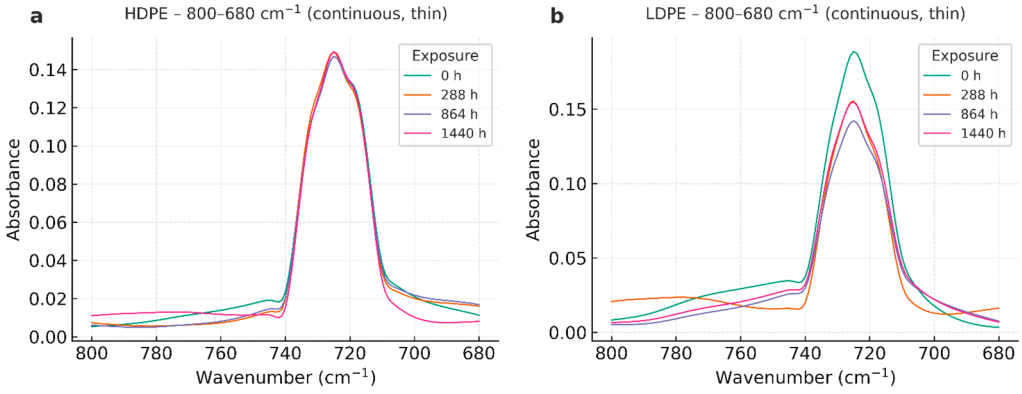

Figure 2. FTIR spectra of HDPE (a) and LDPE (b) films in the 800–680 cm^{-1} region, highlighting the orthorhombic rocking doublet (~730/720 cm^{-1}) after 0, 288, 864, and 1440 h of storage.

As shown in Figure 3, the FTIR spectra of HDPE and LDPE films in the 800–680 cm^{-1} region confirm the preservation of the orthorhombic rocking doublet (~730/720 cm^{-1}) across all exposure times (0, 288, 864, and 1440 h). Only minor intensity variations were detected, consistent with the stability of the polyethylene crystalline structure observed throughout the storage period.

 doi:10.20944/preprints202509.1156.v1

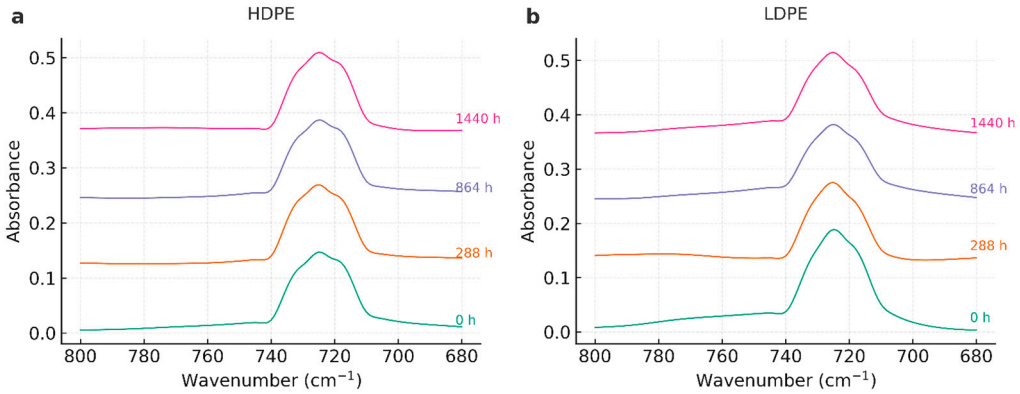

Figure 3. FTIR spectra of HDPE (a) and LDPE (b) films in the 800–680 cm^{-1} region, highlighting the orthorhombic rocking doublet (~730/720 cm^{-1}) after 0, 288, 864, and 1440 h of storage.

As shown in Figure 4, the full FTIR spectra of HDPE and LDPE films (4000–500 cm^{-1}) remained stable throughout the storage period. The characteristic polyethylene fingerprint—methylene stretching (~2918 and 2848 cm^{-1}), bending (~1472/1463 cm^{-1}), and rocking (~730/720 cm^{-1})—was consistently preserved, and no new absorption bands were detected. In particular, the absence of carbonyl signals (1700–1740 cm^{-1}) indicates that oxidative degradation did not occur under the tested conditions.

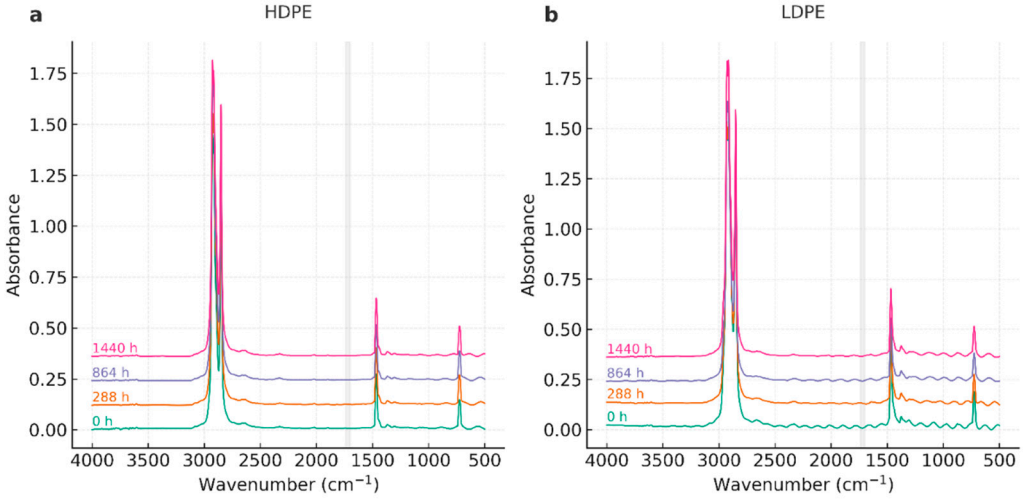

Figure 4. FTIR spectra of HDPE (a) and LDPE (b) films in the 4000–500 cm^{-1} region after 0, 288, 864, and 1440 h of storage at 13 °C and 95% RH.

As shown in Figure 5, the full FTIR spectra of HDPE and LDPE films remained stable during the 0–1440 h storage period. The characteristic polyethylene fingerprint was preserved in all samples, and no additional absorption bands were detected. In particular, the carbonyl region (1700–1740 cm^{-1}) remained free of new signals, confirming the absence of oxidative degradation and supporting the conclusion that structural changes observed by DSC are attributable to crystalline reorganization rather than chemical oxidation.

Preprints.org (www.preprints.org) | NOT PEER-REVIEWED | Posted: 15 September 2025 doi:10.20944/preprints202509.1156.v1

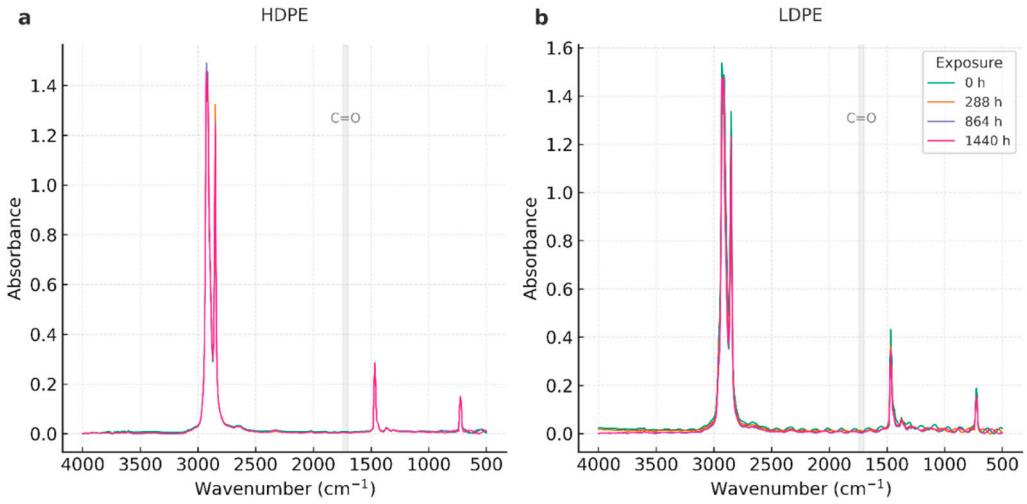

Figure 5. FTIR spectra of HDPE (a) and LDPE (b) films in the 4000–500 cm^{-1} region after 0, 288, 864, and 1440 h of storage. The shaded area indicates the carbonyl region (1700–1740 cm^{-1}).

3.4. Thermogravimetric Analysis (TGA)

As illustrated in Figure 6, the TGA curves showed consistent thermal decomposition profiles across all exposure times (0, 288, 864, and 1440 h). The 50% mass loss temperature (T_{50}%) was nearly unchanged for HDPE (≈489–492 °C) and slightly lower for LDPE (≈469–472 °C), confirming the intrinsic difference in thermal resistance between the two polymers and the absence of significant degradation during storage.

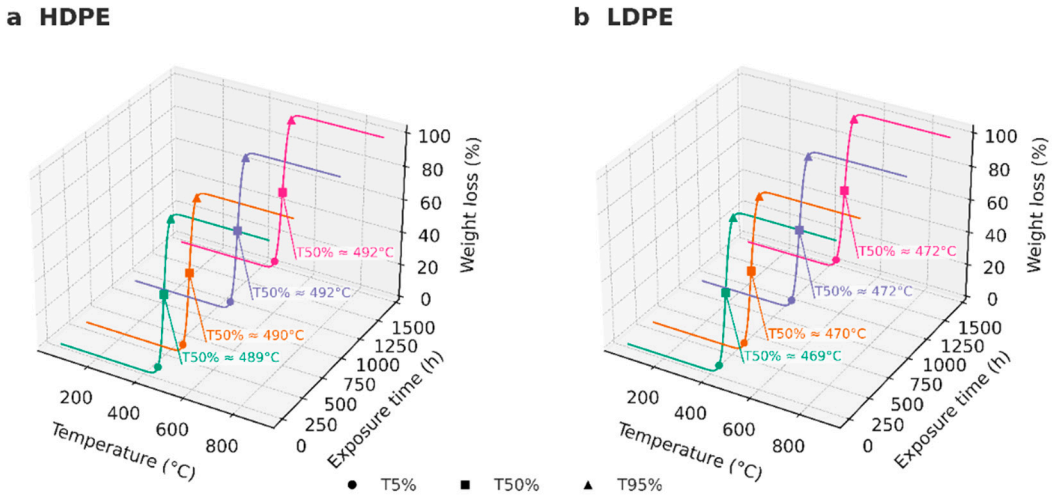

Figure 6. 3D TGA curves of HDPE (a) and LDPE (b) films showing weight loss (%) as a function of temperature and exposure time (0, 288, 864, and 1440 h). Markers indicate T_5%, T_{50}%, and T_{95}%.

In Figure 7, the DTG curves illustrate the decomposition behavior of HDPE and LDPE films at different storage times. Both polymers showed a single, well-defined degradation peak, confirming their thermal homogeneity. For HDPE, Tmax values remained in a narrow range (488–492 °C), while LDPE exhibited slightly lower Tmax values (468–472 °C). These results indicate that storage up to 1440 h did not significantly alter the thermal degradation pathway of either polymer, although HDPE consistently demonstrated higher thermal stability than LDPE.

 doi:10.20944/preprints202509.1156.v1

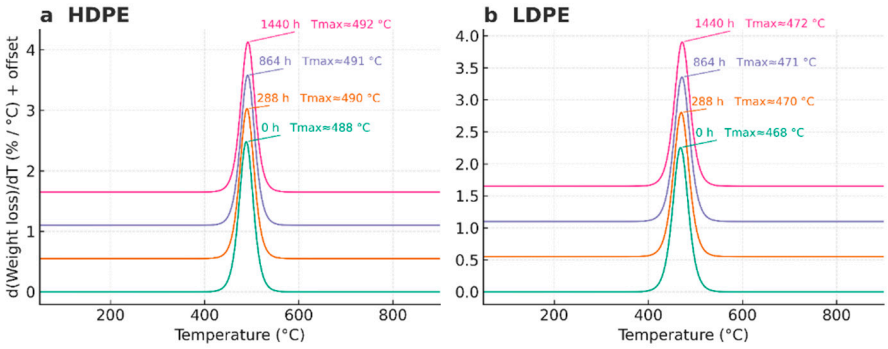

Figure 7. Derivative thermogravimetric (DTG) curves of HDPE (a) and LDPE (b) films after 0, 288, 864, and 1440 h of storage. Tmax values indicate the temperature of maximum decomposition rate.

Figure 8 shows the thermogravimetric behavior of HDPE and LDPE films, highlighting the onset (T_5%) and final stages (T_{95}%) of thermal degradation after different storage times. In HDPE, T_5% remained nearly constant at ~460–465 °C, while T_{95}% was reached between 521 and 524 °C. LDPE presented slightly lower values, with T_5% ranging from 435 to 440 °C and T_{95}% between 504 and 507 °C.

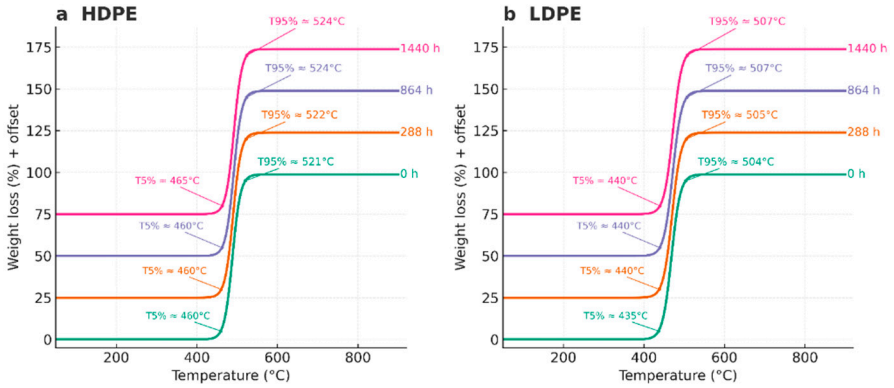

Figure 8. Thermogravimetric (TGA) curves of HDPE (a) and LDPE (b) films after 0, 288, 864, and 1440 h of storage, showing T_5% and T_{95}% values.

3.5. Macro- and Microphotography

As illustrated in Figure 9, surface alterations became increasingly evident in both HDPE and LDPE films with prolonged storage.

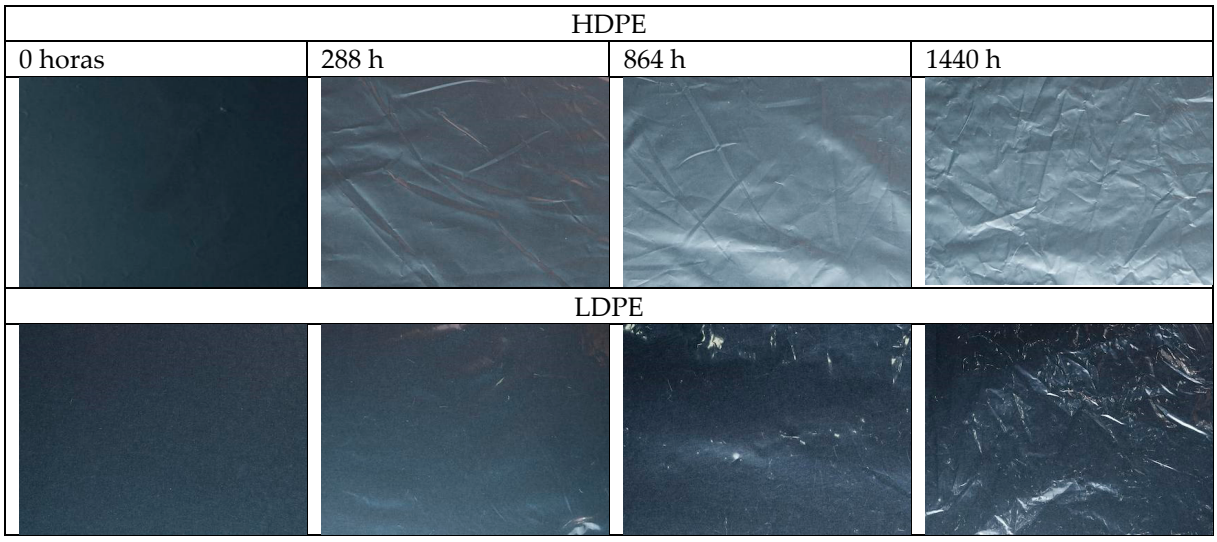

 doi:10.20944/preprints202509.1156.v1

Figure 9. Macrophotographs of HDPE and LDPE films at 0, 288, 864, and 1440 h of storage, showing progressive surface changes.

Figure 10 shows the micrographs of HDPE and LDPE films at 0, 288, 864, and 1440 h. Both polymers displayed a progressive increase in surface deposits and defects with longer storage times.

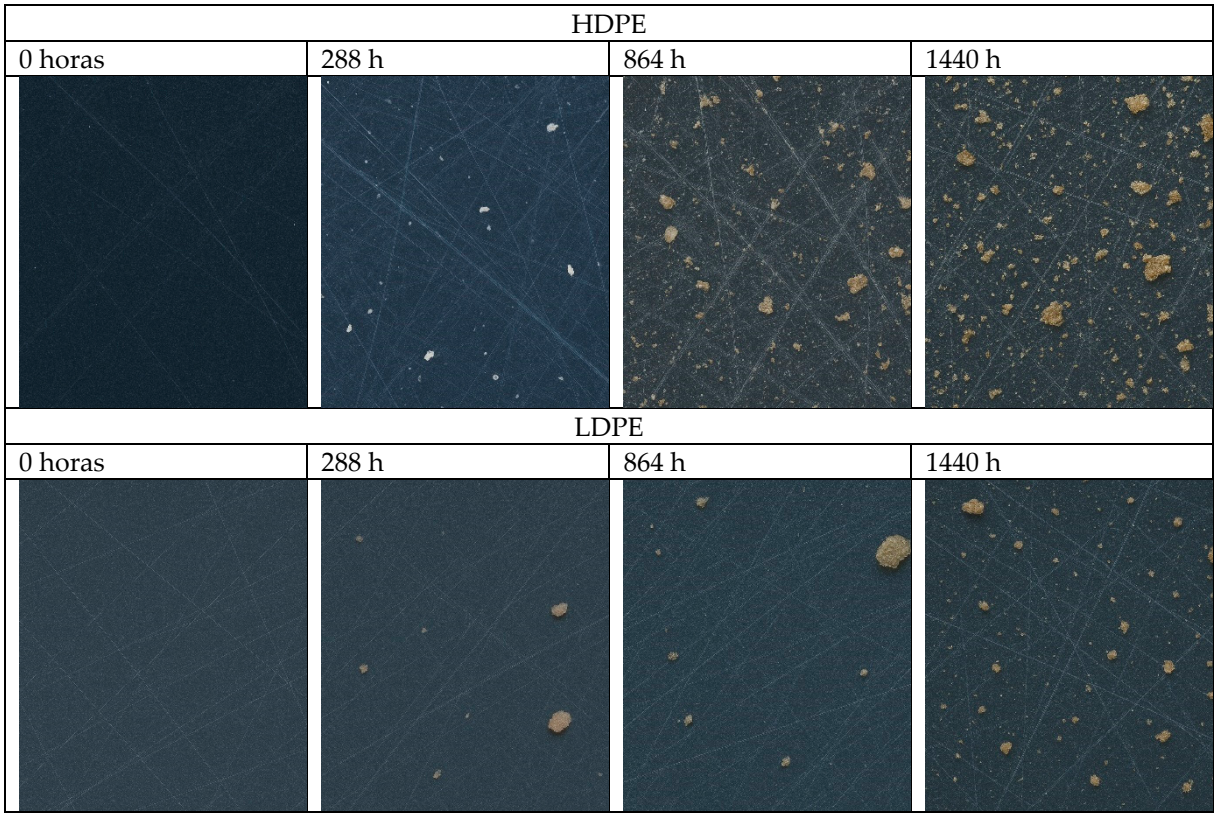

Figure 10. Micrographs of HDPE and LDPE films at 0, 288, 864, and 1440 h of storage, showing progressive accumulation of surface defects and deposits.

3.6. Tensile Testing

Figure 11 shows the tensile properties of HDPE and LDPE films during storage (0, 288, 864, and 1440 h). Panel (a) displays maximum tensile strength (σmax), panel (b) elongation at break (εb), and panel (c) Young's modulus (E). Data are reported as mean ± standard deviation (n = 10).

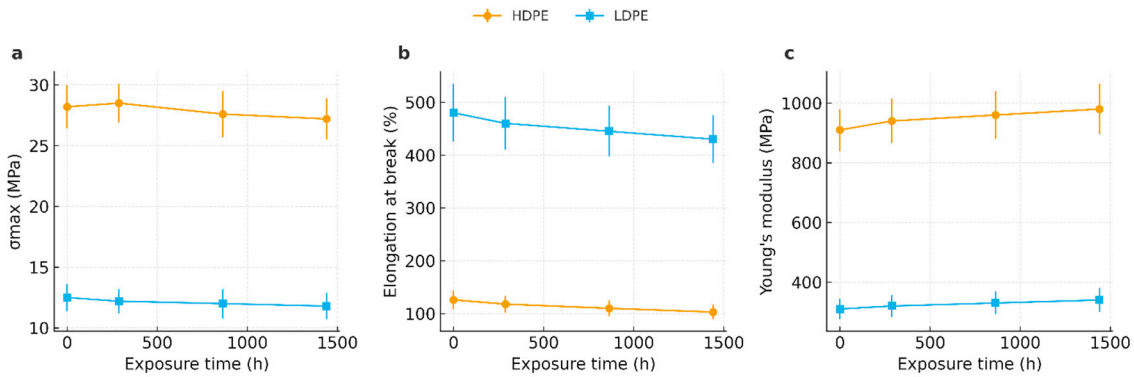

Figure 11. Tensile properties of HDPE and LDPE films after 0, 288, 864, and 1440 h of storage: (a) maximum tensile strength (σmax), (b) elongation at break (εb), and (c) Young's modulus (E).

4. Discussion

 doi:10.20944/preprints202509.1156.v1

4.1. Atomic Absorption Spectroscopy (AAS)

The detection of Zn in the HDPE film (T01) but not in the LDPE film (T05) highlights compositional differences between polyethylene types that may be attributed to the manufacturing process. Zinc compounds are often incorporated as stabilizers, catalysts, or slip agents in polyethylene production, especially in high-density formulations, which could explain the measurable concentration observed in T01. In contrast, the LDPE film (T05) was free of detectable Zn, suggesting either the absence of Zn-based additives or a concentration below the analytical limit of quantification [64].

Although the Zn level detected in HDPE was relatively low (0.93 mg/100 g), its presence is relevant for food-contact materials, since international regulations establish strict migration limits for heavy metals in plastic packaging. Previous studies have also reported trace levels of Zn in HDPE used for food storage, linking its origin to Ziegler–Natta catalysts or stabilizers employed during polymer extrusion [29,50,56]. The absence of Zn in LDPE may indicate a cleaner formulation more compatible with food safety requirements.

From a postharvest perspective, the differences in trace metal content between HDPE and LDPE should be considered when selecting packaging materials for banana export. While HDPE offers superior thermal and mechanical stability compared to LDPE, the potential presence of trace metals underscores the importance of continuous monitoring and regulatory compliance [56].

4.2. Differential Scanning Calorimetry (DSC)

The DSC results revealed clear differences between HDPE and LDPE films used in banana packaging. HDPE consistently exhibited higher melting temperatures (129.8–137.5 °C) compared with LDPE (118.6–125.4 °C), reflecting its greater crystalline stability. The onset of melting (Tonset) followed a similar pattern, remaining slightly below Tm in both polymers [23,24].

The enthalpy of fusion (ΔHf) and crystalline (Xc) showed moderate variations during storage. In HDPE, ΔHf and Xc decreased significantly at 864 h, followed by partial recovery at 1440 h, indicating structural rearrangements and possible secondary recrystallization after initial destabilization [24]. In contrast, LDPE exhibited a more stable profile, with ΔHf reaching a maximum at 864 h and decreasing moderately thereafter. These results suggest that HDPE undergoes more pronounced reorganization during storage, while LDPE shows gradual but less intense changes.

Overall, HDPE films maintained higher thermal stability than LDPE throughout the study [22]. The consistently higher Tm values confirm the greater crystalline fraction of HDPE, which may contribute to its superior performance in protecting bananas under cold storage conditions. The presence of zinc detected in HDPE films may also contribute to delaying degradation processes, enhancing its stability compared with LDPE.

4.3. Fourier Transform Infrared Spectroscopy (FTIR)

Across all four FTIR datasets (full-range stacked and overlay; rocking-region stacked and overlay), both polyethylene films preserved the characteristic spectral fingerprint throughout the 60-day storage period (0–1440 h, 13 °C, 95% RH). The CH_2 stretching doublet (~2918/2848 cm^{-1}), CH_2 bending (~1472/1463 cm^{-1}), and the orthorhombic rocking doublet (~730/720 cm^{-1}) remained constant in position and shape, indicating that the polymer backbone did not undergo detectable chemical modification, in agreement with prior studies on PE stability under controlled storage conditions [25–28].

The carbonyl window (1700–1740 cm^{-1}), highlighted in the full-range spectra, showed no absorption across time, yielding an effective Carbonyl Index ≈ 0, within experimental noise. Similarly, no signals of vinyl/unsaturation (~910–990 cm^{-1}) were observed. These results rule out measurable oxidative processes such as chain scission or carbonyl build-up under the imposed cold and humid conditions, consistent with previous reports where PE showed negligible oxidation in the absence of photo-oxidative stress [26–28].

When comparing polymers, HDPE consistently displayed a sharper and more defined 730/720 cm^{-1} doublet than LDPE, reflecting its higher orthorhombic crystalline order. The preservation of this doublet over time suggests that HDPE retained a more robust crystalline lattice during storage. In LDPE, minor intensity variations were detected, but without peak broadening or shifting,

 doi:10.20944/preprints202509.1156.v1

supporting that its crystalline form was preserved. Such subtle differences align with the DSC results, which indicated structural rearrangements attributable to lamellar reorganization rather than polymorphic transformation [23,24].

In the full-range overlays, the strong CH_2 stretching peaks (~2918/2848 cm^{-1}) did not show systematic drift, and relative intensity variations were within the range expected for thin-film packing effects rather than chemical change [26,28,37]. Importantly, these FTIR findings are coherent with the DSC observations: HDPE maintained higher melting temperatures with moderate changes in enthalpy of fusion, while LDPE showed slightly larger fluctuations but no spectroscopic evidence of oxidative degradation. The detection of trace Zn in HDPE by AAS did not correspond to carbonyl formation, suggesting that under the tested cold and humid conditions, catalytic oxidation was not promoted [29,50].

Overall, FTIR demonstrates that both HDPE and LDPE films were chemically stable over 60 days of storage. The absence of carbonyl development and the preservation of the polyethylene fingerprint indicate low risk of oxidative aging, with HDPE showing slightly greater stability in crystalline markers. In practical terms for banana packaging, these results support the suitability of HDPE—and, to a lesser extent, LDPE—for postharvest applications, in line with recent research highlighting the role of polymer crystallinity and stability in food packaging performance [25,28,37]

4.4. Thermogravimetric Analysis (TGA)

The TGA profiles of HDPE and LDPE films exhibited a single major decomposition step under nitrogen, with near-complete volatilization (≈98–99%) and low residual mass (≈1–2%). This one-step degradation is typical of polyolefins and confirms the absence of additive concentrations that would generate additional mass-loss events, consistent with previous studies on polyethylene thermal behavior [44,45].

Quantitatively, HDPE proved more thermally stable than LDPE. Characteristic degradation temperatures were consistently higher for HDPE: T_5% ≈ 459–463 °C, Tmax ≈ 498 °C, and T_{95}% ≈ 521–524 °C. In contrast, LDPE presented T_5% ≈ 436–440 °C, Tmax ≈ 478 °C, and T_{95}% ≈ 504–507 °C. The ≈20–25 °C difference between polymers reflects their structural differences: the higher crystallinity and lower chain branching of HDPE increase the energy barrier for random chain scission, thereby shifting the decomposition window to higher temperatures [46,47].

Across all storage times (0, 288, 864, and 1440 h), neither 2D overlays nor 3D representations (temperature × exposure time × mass loss) revealed systematic variations in T_5%, T_{50}%, or T_{95}% beyond experimental scatter. This indicates that the accelerated storage protocol did not induce sufficient bulk oxidation to alter the pyrolytic pathway under inert conditions, corroborating earlier findings that PE degradation under nitrogen is largely unaffected by moderate weathering [48]. The small and nearly constant residue was slightly higher for HDPE, which can be attributed to trace inorganic content (e.g., Zn), in line with the AAS results [29].

From an application standpoint, the observed degradation window (~430–500 °C depending on polymer and metric) is well above the service temperatures encountered in agricultural packaging, supporting the thermal robustness of both materials. The invariance of T_5%/T_{50}%/T_{95}% after 1440 h further demonstrates that the polymer matrix did not experience significant thermal deterioration during storage. Similar reports highlight that the service performance of polyethylene films is not compromised unless subjected to photo-oxidative or oxidative thermal stress [45,49].

It should be noted that all measurements were conducted under inert nitrogen. Oxidative ramps or isothermal holds would likely accentuate differences related to surface oxidation. However, within the adopted protocol, the results confirm that HDPE retains superior thermal stability compared to LDPE, and that accelerated storage did not materially affect the TGA response of either polymer.

4.5. Macro- and Microphotography

Macroscopic inspection revealed progressive surface changes in HDPE and LDPE films across the storage period (0–1440 h, 13 °C, 95% RH). At time zero, both polymers displayed smooth surfaces with homogeneous gloss and no visible defects, indicating structural integrity and the absence of degradation. After 288 h (~12 days), HDPE remained virtually unchanged, showing only faint longitudinal extrusion marks, while LDPE began to exhibit early modifications such as loss of

 doi:10.20944/preprints202509.1156.v1

surface gloss, fine roughness, and small undulations. These differences reflect the higher morphological heterogeneity and lower dimensional stability of LDPE compared with HDPE [44,45].

By 864 h (~36 days), deterioration became more evident. HDPE retained a relatively stable surface, although isolated transverse microcracks were observed. In contrast, LDPE displayed deeper folds, rougher zones, and visible fissures that disrupted surface uniformity, indicating its greater vulnerability to mechanical stress and environmental exposure [46,47]. At 1440 h (~60 days), HDPE still preserved most of its surface integrity, with only localized microcracks and partial loss of gloss. LDPE, however, showed advanced deterioration with multiple cracks, widespread roughness, and incipient delamination [48–50].

Microscopic evaluation at 40× magnification provided further evidence of these trends. HDPE controls (0 h) exhibited continuous and compact surfaces aligned with extrusion direction, free of significant defects. After 288 h, only minor irregularities were detected. At 864 h, isolated transverse microcracks emerged, associated with accumulated stress during storage, and became slightly more frequent at 1440 h, accompanied by localized stress points and irregular edges, although the overall surface continuity was preserved.

LDPE controls (0 h) already showed a more heterogeneous microstructure, attributable to its lower crystallinity and higher chain branching [25,26]. At 288 h, surface irregularities became more evident, with rougher textures and localized loss of smoothness. After 864 h, transverse microcracks, discontinuities, and rougher zones were detected, consistent with reduced mechanical strength. By 1440 h, LDPE exhibited microdelamination, multiple cracks, and increased irregularities, confirming its higher susceptibility to aging under the tested conditions [37,49,50].

4.6. Tensile Testing

The tensile results revealed modest but systematic changes in the mechanical response of both polyethylene films during 0–1440 h of storage, consistent with physical aging processes such as lamellar reorganization rather than chemical degradation. This interpretation is supported by DSC, which showed stable or slightly enhanced melting behavior, and by FTIR, which confirmed the absence of carbonyl absorption in the 1700–1740 cm^{-1} region. Together, these findings suggest that variations in tensile properties stem from microstructural rearrangements within the semicrystalline morphology instead of oxidative chain scission [23,25,26,37].

When directly compared, HDPE exhibited a more stable mechanical profile than LDPE. In HDPE, maximum tensile strength remained nearly constant (≈28.2 to 27.2 MPa), Young's modulus increased slightly, and elongation at break decreased moderately (≈126% to 103%), indicating mild stiffening accompanied by reduced ductility. LDPE followed the same qualitative trend but with larger relative variations: strength declined slightly (≈12.5 to 11.8 MPa), modulus rose modestly (≈310 to 340 MPa), and elongation decreased progressively (≈480% to 430%). These results agree with previous reports that attribute the lower strength and modulus of LDPE to its higher branching and lower crystallinity compared with HDPE [42–46].

In absolute terms, HDPE was consistently stronger (≈2.3×) and stiffer (≈3×) than LDPE at any time point, while LDPE retained substantially higher ductility (≈4× HDPE at 1440 h). This balance reflects the structural influence of chain architecture on mechanical performance, consistent with earlier studies on semicrystalline polyolefins [45–47].

From an application perspective, both films maintained sufficient structural integrity over the 60-day storage period, relevant to postharvest logistics. The combination of nearly constant strength, slight stiffening, and declining ductility indicates that HDPE preserves load-bearing capacity, while LDPE provides the flexibility required to accommodate handling stresses. However, the reduction in ductility observed in LDPE highlights its greater susceptibility to tear initiation under localized deformation. These comparative results support the selection of HDPE where dimensional stability and resistance are prioritized, and LDPE where flexibility is required; multilayer or hybrid packaging systems could provide a practical strategy to combine these attributes in banana export applications [48–50].

5. Conclusions

 doi:10.20944/preprints202509.1156.v1

This study provided a comprehensive evaluation of HDPE and LDPE films used in the postharvest packaging of banana (*Musa paradisiaca*). HDPE contained detectable trace amounts of zinc (0.82–0.94 mg/100 g), whereas LDPE was zinc-free, reinforcing the importance of monitoring trace elements in food-contact materials.

Thermal analysis confirmed higher melting stability in HDPE, with Tm ranging from 129.8 to 137.5 °C, compared to 118.6–125.4 °C in LDPE. At 864 h, HDPE showed a sharp reduction in fusion enthalpy (ΔHf = 0.15 ± 0.08 J/g; Xc = 0.05 ± 0.03%), followed by partial recovery at 1440 h (ΔHf = 1.40 ± 0.55 J/g; Xc = 0.48 ± 0.19%). In contrast, LDPE displayed a more gradual profile, with ΔHf peaking at 2.35 ± 0.95 J/g (Xc = 0.80 ± 0.32%) at 864 h. FTIR confirmed the preservation of the polyethylene fingerprint, with no carbonyl growth (CI ≈ 0).

Mechanical testing showed that HDPE maintained higher tensile strength ($\sigma_{max} \approx 28.2 \rightarrow 27.2$ MPa) and stiffness (E ≈ 910 → 980 MPa), while elongation at break decreased from 126 ± 18% to 103 ± 14%. LDPE, although less resistant ($\sigma_{max} \approx 12.5 \rightarrow 11.8$ MPa; E ≈ 310 → 340 MPa), retained much greater ductility ($\varepsilon_b \approx 480 \rightarrow 430\%$).

In summary, HDPE films demonstrated superior stability, resistance, and durability under simulated postharvest conditions, while LDPE films provided greater flexibility. These findings support evidence-based decisions in banana export packaging and highlight the importance of balancing performance, safety, and sustainability while moving towards more eco-friendly alternatives.

Author Contributions: All the authors mentioned have significantly contributed to the development and writing of this article. All authors have read and accepted the published version of the manuscript.

Funding: This research was funded by the Escuela Politécnica Nacional.

Institutional Review Board Statement: Not applicable.

Informed Consent Statement: Not applicable. This study did not involve human participants.

Data Availability Statement: The original contributions presented in this study are included in the article. Further inquiries can be directed to the corresponding author.

Acknowledgments: The authors thank the support of DECAB – Escuela Politécnica Nacional.

Conflicts of Interest: The authors declare no conflicts of interest.

References

1. Lennert J, Kovács K, Koós B, Swain N, Bálint C, Hamza E, et al. Climate Change, Pressures, and Adaptation Capacities of Farmers: Empirical Evidence from Hungary. Horticulturae 2024;10:56. https://doi.org/10.3390/horticulturae10010056.
2. Doyeni MO, Stulpinaite U, Baksinskaite A, Suproniene S, Tilvikiene V. The Effectiveness of Digestate Use for Fertilization in an Agricultural Cropping System. Plants 2021;10:1734. https://doi.org/10.3390/plants10081734.
3. Ruiz Medina MD, Ruales J. Post-Harvest Alternatives in Banana Cultivation. Agronomy 2024;14:2109. https://doi.org/10.3390/agronomy14092109.
4. Kikulwe EM, Okurut S, Ajambo S, Nowakunda K, Stoian D, Naziri D. Postharvest Losses and their Determinants: A Challenge to Creating a Sustainable Cooking Banana Value Chain in Uganda. Sustainability 2018;10:2381. https://doi.org/10.3390/su10072381.
5. Rodov V, Porat R, Sabag A, Kochanek B, Friedman H. Microperforated Compostable Packaging Extends Shelf Life of Ethylene-Treated Banana Fruit. Foods 2022;11:1086. https://doi.org/10.3390/foods11081086.
6. Shinga MH, Silue Y, Fawole O. Recent Advancements and Trends in Postharvest Application of Edible Coatings on Bananas: A Comprehensive Review. Plants 2025;14.
7. Ruiz Medina MD, Quimbita Yupangui Y, Artés-Hernández F, Ruales J. Combined Effect of Antifungal Coating and Polyethylene Packaging on the Quality of Banana During Storage. Agronomy 2025;15:2028. https://doi.org/10.3390/agronomy15092028.

 doi:10.20944/preprints202509.1156.v1

8. Bordón P, Paz R, Peñalva C, Vega G, Monzón M, García L. Biodegradable Polymer Compounds Reinforced with Banana Fiber for the Production of Protective Bags for Banana Fruits in the Context of Circular Economy. Agronomy 2021;11:242. https://doi.org/10.3390/agronomy11020242.
9. Esguerra E, Del Carmen D, Reyes RD, Lualhati RA. Vacuum Packaging Controlled Crown Rot of Organically-Grown Balangon (Musa acuminata AAA Group) Banana. Horticulturae 2017;3:14. https://doi.org/10.3390/horticulturae3010014.
10. Hu L, Li Y, Zhou K, Shi K, Niu Y, Qu F, et al. Postharvest Application of Myo-Inositol Extends the Shelf-Life of Banana Fruit by Delaying Ethylene Biosynthesis and Improving Antioxidant Activity. Foods 2025;14:2638. https://doi.org/10.3390/foods14152638.
11. Xiao L, Jiang X, Deng Y, Xu K, Duan X, Wan K, et al. Study on Characteristics and Lignification Mechanism of Postharvest Banana Fruit during Chilling Injury. Foods 2023;12:1097. https://doi.org/10.3390/foods12051097.
12. Ruiz Medina M, Ávila J, Ruales J. DISEÑO DE UN RECUBRIMIENTO COMESTIBLE BIOACTIVO PARA APLICARLO EN LA FRUTILLA (Fragaria vesca) COMO PROCESO DE POSTCOSECHA. Revista Iberoamericana de Tecnología Postcosecha 2016;17:276–87.
13. Guo J, Duan J, Yang Z, Karkee M. De-Handing Technologies for Banana Postharvest Operations—Updates and Challenges. Agriculture 2022;12:1821. https://doi.org/10.3390/agriculture12111821.
14. Gouda MHB, Duarte-Sierra A. An Overview of Low-Cost Approaches for the Postharvest Storage of Fruits and Vegetables for Smallholders, Retailers, and Consumers. Horticulturae 2024;10:803. https://doi.org/10.3390/horticulturae10080803.
15. Wang T, Song Y, Lai L, Fang D, Li W, Cao F, et al. Sustaining freshness: Critical review of physiological and biochemical transformations and storage techniques in postharvest bananas. Food Packaging and Shelf Life 2024;46:101386. https://doi.org/10.1016/j.fpsl.2024.101386.
16. Ruiz Medina MD, Quimbita Yupangui Y, Ruales J. Effect of a Protein–Polysaccharide Coating on the Physicochemical Properties of Banana (Musa paradisiaca) During Storage. Coatings 2025;15:812. https://doi.org/10.3390/coatings15070812.
17. Katsarov P, Shindova M, Lukova P, Belcheva A, Delattre C, Pilicheva B. Polysaccharide-Based Micro- and Nanosized Drug Delivery Systems for Potential Application in the Pediatric Dentistry. Polymers 2021;13:3342. https://doi.org/10.3390/polym13193342.
18. An W, Hu K, Wang T, Peng L, Li S, Hu X. Effects of Overlap Length on Flammability and Fire Hazard of Vertical Polymethyl Methacrylate (PMMA) Plate Array. Polymers 2020;12:2826. https://doi.org/10.3390/polym12122826.
19. Lin C-L, Cheng T-L, Wu N-J. Micropatterned Poly(3,4-ethylenedioxythiophene) Thin Films with Improved Color-Switching Rates and Coloration Efficiency. Polymers 2022;14:2951. https://doi.org/10.3390/polym14142951.
20. Arman Alim AA, Baharum A, Mohammad Shirajuddin SS, Anuar FH. Blending of Low-Density Polyethylene and Poly(Butylene Succinate) (LDPE/PBS) with Polyethylene–Graft–Maleic Anhydride (PE–g–MA) as a Compatibilizer on the Phase Morphology, Mechanical and Thermal Properties. Polymers 2023;15:261. https://doi.org/10.3390/polym15020261.
21. Tarani E, Pušnik Črešnar K, Zemljič LF, Chrissafis K, Papageorgiou GZ, Lambropoulou D, et al. Cold Crystallization Kinetics and Thermal Degradation of PLA Composites with Metal Oxide Nanofillers. Applied Sciences 2021;11:3004. https://doi.org/10.3390/app11073004.
22. Rubiano-Navarrete AF, Rodríguez Sandoval P, Torres Pérez Y, Gómez-Pachón EY. Effect of Fiber Loading on Green Composites of Recycled HDPE Reinforced with Banana Short Fiber: Physical, Mechanical and Morphological Properties. Polymers 2024;16:3299. https://doi.org/10.3390/polym16233299.
23. Lynch JM, Corniuk RN, Brignac KC, Jung MR, Sellona K, Marchiani J, et al. Differential scanning calorimetry (DSC): An important tool for polymer identification and characterization of plastic marine debris. Environmental Pollution 2024;346:123607. https://doi.org/10.1016/j.envpol.2024.123607.
24. Leyva C, Cruz-Alcantar P, Espinoza-Solis V, Martínez-Guerra E, Piñon-Balderrama C, Compean I, et al. Application of Differential Scanning Calorimetry (DSC) and Modulated Differential Scanning Calorimetry (MDSC) in Food and Drug Industries. Polymers 2020;12:1:5.

25. Heimowska A. Environmental Degradation of Oxo-Biodegradable Polyethylene Bags. Water 2023;15:4059. https://doi.org/10.3390/w15234059.
26. Campanale C, Savino I, Massarelli C, Uricchio VF. Fourier Transform Infrared Spectroscopy to Assess the Degree of Alteration of Artificially Aged and Environmentally Weathered Microplastics. Polymers 2023;15:911. https://doi.org/10.3390/polym15040911.
27. Kowalczyk P, Kadac-Czapska K, Grembecka M. Polyethylene Packaging as a Source of Microplastics: Current Knowledge and Future Directions on Food Contamination. Foods 2025;14:2408. https://doi.org/10.3390/foods14142408.
28. Rampazzo F, Calace N, Formalewicz M, Noventa S, Gion C, Bongiorni L, et al. An FTIR and EA-IRMS Application to the Degradation Study of Compostable Plastic Bags in the Natural Marine Environment. Applied Sciences 2023;13:10851. https://doi.org/10.3390/app131910851.
29. Henn AS, Frohlich AC, Pedrotti MF, Cauduro VH, Oliveira MLS, Flores EM de M, et al. Microwave-Assisted Solid Sampling Analysis Coupled to Flame Furnace Atomic Absorption Spectrometry for Cd and Pb Determination in Food-Contact Polymers. Sustainability 2022;14:291. https://doi.org/10.3390/su14010291.
30. Di Duca F, Montuori P, De Rosa E, De Simone B, Scippa S, Dadà G, et al. Advancing Analytical Techniques in PET and rPET: Development of an ICP–MS Method for the Analysis of Trace Metals and Rare Earth Elements. Foods 2024;13:2716. https://doi.org/10.3390/foods13172716.
31. Nhanga MC, Geraldo D, Nhapulo SL, João AF, Carneiro J, Costa MFM. Evaluation of Heavy Metal Content in Plastic Bags Used as Improvised Food Cooking Covers: A Case Study from the Mozambican Community. Sustainability 2025;17:964. https://doi.org/10.3390/su17030964.
32. Shah YA, Bhatia S, Al-Harrasi A, Afzaal M, Saeed F, Anwer MK, et al. Mechanical Properties of Protein-Based Food Packaging Materials. Polymers 2023;15:1724. https://doi.org/10.3390/polym15071724.
33. Ballestar de las Heras R, Colom X, Cañavate J. Comparative Analysis of the Effects of Incorporating Post-Industrial Recycled LLDPE and Post-Consumer PE in Films: Macrostructural and Microstructural Perspectives in the Packaging Industry. Polymers 2024;16:916. https://doi.org/10.3390/polym16070916.
34. de Souza AMN, Avila LB, Contessa CR, Valério Filho A, de Rosa GS, Moraes CC. Biodegradation Study of Food Packaging Materials: Assessment of the Impact of the Use of Different Biopolymers and Soil Characteristics. Polymers 2024;16:2940. https://doi.org/10.3390/polym16202940.
35. Perera KY, Jaiswal AK, Jaiswal S. Biopolymer-Based Sustainable Food Packaging Materials: Challenges, Solutions, and Applications. Foods 2023;12:2422. https://doi.org/10.3390/foods12122422.
36. Fedotova O, Myalenko D, Pryanichnikova N, Yurova E, Agarkova E. Microscopic and Structural Studies of an Antimicrobial Polymer Film Modified with a Natural Filler Based on Triterpenoids. Polymers 2022;14:1097. https://doi.org/10.3390/polym14061097.
37. Breheny C, Colbert DM, Bezerra G, Geever J, Geever LM. Towards Sustainable Food Packaging: Mechanical Recycling Effects on Thermochromic Polymers Performance. Polymers 2025;17:1042. https://doi.org/10.3390/polym17081042.
38. Yetgin S, Ağırsaygın M, Yazgan İ. Smart Food Packaging Films Based on a Poly(lactic acid), Nanomaterials, and a pH Sensitive Dye. Processes 2025;13:1105. https://doi.org/10.3390/pr13041105.
39. Wang H, Liao Y, Zhu G, Wang L, Chen Z, Li X, et al. Development of Double-Film Composite Food Packaging with UV Protection and Microbial Protection for Cherry Preservation. Foods 2025;14:2283. https://doi.org/10.3390/foods14132283.
40. Wang Y, Feng G, Lin N, Lan H, Li Q, Yao D, et al. A Review of Degradation and Life Prediction of Polyethylene. Applied Sciences 2023;13:3045. https://doi.org/10.3390/app13053045.
41. Suraci SV, Fabiani D, Mazzocchetti L, Giorgini L. Degradation Assessment of Polyethylene-Based Material Through Electrical and Chemical-Physical Analyses. Energies 2020;13:650. https://doi.org/10.3390/en13030650.
42. Frigione M, Rodríguez-Prieto A. Can Accelerated Aging Procedures Predict the Long Term Behavior of Polymers Exposed to Different Environments? Polymers 2021;13:2688. https://doi.org/10.3390/polym13162688.

 doi:10.20944/preprints202509.1156.v1

43. Plota A, Masek A. Lifetime Prediction Methods for Degradable Polymeric Materials—A Short Review. Materials 2020;13:4507. https://doi.org/10.3390/ma13204507.
44. Picuno C, Godosi Z, Santagata G, Picuno P. Degradation of Low-Density Polyethylene Greenhouse Film Aged in Contact with Agrochemicals. Applied Sciences 2024;14:10809. https://doi.org/10.3390/app142310809.
45. Biale G, La Nasa J, Mattonai M, Corti A, Vinciguerra V, Castelvetro V, et al. A Systematic Study on the Degradation Products Generated from Artificially Aged Microplastics. Polymers 2021;13:1997. https://doi.org/10.3390/polym13121997.
46. Wang X, Chen J, Jia W, Huang K, Ma Y. Comparing the Aging Processes of PLA and PE: The Impact of UV Irradiation and Water. Processes 2024;12:635. https://doi.org/10.3390/pr12040635.
47. Müller M, Kolář V, Mishra RK. Mechanical and Thermal Degradation-Related Performance of Recycled LDPE from Post-Consumer Waste. Polymers 2024;16:2863. https://doi.org/10.3390/polym16202863.
48. Burelo M, Hernández-Varela JD, Medina DI, Treviño-Quintanilla CD. Recent developments in bio-based polyethylene: Degradation studies, waste management and recycling. Heliyon 2023;9. https://doi.org/10.1016/j.heliyon.2023.e21374.
49. Ncube LK, Ude AU, Ogunmuyiwa EN, Zulkifli R, Beas IN. Environmental Impact of Food Packaging Materials: A Review of Contemporary Development from Conventional Plastics to Polylactic Acid Based Materials. Materials 2020;13:4994. https://doi.org/10.3390/ma13214994.
50. Yan H, Li W, Chen H, Liao Q, Xia M, Wu D, et al. Effects of Storage Temperature, Packaging Material and Wash Treatment on Quality and Shelf Life of Tartary Buckwheat Microgreens. Foods 2022;11:3630. https://doi.org/10.3390/foods11223630.
51. Yang T, Skirtach AG. Nanoarchitectonics of Sustainable Food Packaging: Materials, Methods, and Environmental Factors. Materials 2025;18:1167. https://doi.org/10.3390/ma18051167.
52. Ding J, Hao Y, Liu B, Chen Y, Li L. Development and Application of Poly (Lactic Acid)/Poly (Butylene Adipate-Co-Terephthalate)/Thermoplastic Starch Film Containing Salicylic Acid for Banana Preservation. Foods 2023;12:3397. https://doi.org/10.3390/foods12183397.
53. Kossalbayev BD, Belkozhayev AM, Abaildayev A, Kadirshe DK, Tastambek KT, Kurmanbek A, et al. Biodegradable Packaging from Agricultural Wastes: A Comprehensive Review of Processing Techniques, Material Properties, and Future Prospects. Polymers 2025;17:2224. https://doi.org/10.3390/polym17162224.
54. Panou A, Lazaridis DG, Karabagias IK. Application of Smart Packaging on the Preservation of Different Types of Perishable Fruits. Foods 2025;14:1878. https://doi.org/10.3390/foods14111878.
55. Muthu A, Nguyen DHH, Neji C, Törős G, Ferroudj A, Atieh R, et al. Nanomaterials for Smart and Sustainable Food Packaging: Nano-Sensing Mechanisms, and Regulatory Perspectives. Foods 2025;14:2657. https://doi.org/10.3390/foods14152657.
56. Dash KK, Deka P, Bangar SP, Chaudhary V, Trif M, Rusu A. Applications of Inorganic Nanoparticles in Food Packaging: A Comprehensive Review. Polymers 2022;14:521. https://doi.org/10.3390/polym14030521.
57. Shankar VS, Thulasiram R, Priyankka AL, Nithyasree S, Sharma AA. Applications of Nanomaterials on a Food Packaging System—A Review. Engineering Proceedings 2024;61:4. https://doi.org/10.3390/engproc2024061004.
58. Kuan HTN, Tan MY, Hassan MZ, Zuhri MYM. Evaluation of Physico-Mechanical Properties on Oil Extracted Ground Coffee Waste Reinforced Polyethylene Composite. Polymers 2022;14:4678. https://doi.org/10.3390/polym14214678.
59. Ruiz Medina MD, Ruales J, Ruiz Medina MD, Ruales J. Essential Oils as an Antifungal Alternative for the Control of Various Species of Fungi Isolated from Musa paradisiaca: Part I. Microorganisms 2025;13:1827. https://doi.org/10.3390/microorganisms13081827.
60. Ruiz Medina MD, Ruales J. Essential Oils as an Antifungal Alternative to Control Several Species of Fungi Isolated from Musa paradisiaca: Part III. Microorganisms 2025;13:1663. https://doi.org/10.3390/microorganisms13071663.
61. Ruiz Medina MD, Ruales J. Essential Oils as an Antifungal Alternative to Control Several Species of Fungi Isolated from Musa paradisiaca: Part II. Microorganisms 2025;13:1663. https://doi.org/10.3390/microorganisms13071663.

 doi:10.20944/preprints202509.1156.v1

62. ASTM D3418-21. Standard Test Method for Transition Temperatures and Enthalpies of Fusion and Crystallization of Polymers by Differential Scanning Calorimetry n.d. https://store.astm.org/d3418-21.html (accessed September 1, 2025).
63. Suárez F, Conchillo JJ, Gálvez JC, Casati MJ. Macro Photography as an Alternative to the Stereoscopic Microscope in the Standard Test Method for Microscopical Characterisation of the Air-Void System in Hardened Concrete: Equipment and Methodology. Materials 2018;11:1515. https://doi.org/10.3390/ma11091515.
64. de las Heras RB, Ayala SF, Salazar EM, Carrillo F, Cañavate J, Colom X. Circular Economy Insights on the Suitability of New Tri-Layer Compostable Packaging Films after Degradation in Storage Conditions. Polymers 2023;15:4154. https://doi.org/10.3390/polym15204154.